Nuclear Magnetic Resonance and Conformational Energy Characterization of Repeat Peptides of Elastin: The Cyclohexadecapeptide, *cyclo*-(L-Val_1-L-Pro_2-Gly_3-Gly_4)$_4$

M. A. Khaled,† K. U. Prasad, C. M. Venkatachalam, and D. W. Urry*

Contribution from the Laboratory of Molecular Biophysics, School of Medicine, University of Alabama at Birmingham, Birmingham, Alabama 35294. *Received May 3, 1985*

Abstract: The cyclohexadecapeptide *cyclo*-(L-Val_1-L-Pro_2-Gly_3-Gly_4)$_4$ is synthesized and its conformational characteristics, in solution, are derived by employing ^1H and ^{13}C NMR methods. Selective decoupling and ^{13}C $\{^1H\}$ NOE are used to assign the ^1H and ^{13}C resonances in particular to delineate the two glycine residues in the molecule. Temperature and solvent dependence of peptide N*H* chemical shift are used to evaluate secondary structure. The dominant conformational feature of this molecule is shown to be a recurring type II β turn utilizing a hydrogen bond between the Gly_4NH and Val_1 C=O groups. T_1 values demonstrate increased flexibility of the chain segment, Gly_4-Val_1, which connects the β-turns. Comparable conformational features were also obtained by using in vacuo conformational energy calculations. The conformational properties of this cyclic molecule show a close relationship to its linear counterpart. The overall conformational behavior of the tetramer series is compared with the pentamer series, L-Val_1-L-Pro_2-Gly_3-L-Val_4-Gly_5, of elastin, particularly in terms of librations within the chain segments, Val_4-Gly_5-Val_1 and Gly_4-Val_1, connecting the β-turns. In analogy to the polypentapeptide study wherein a new mechanism of elasticity was developed, the present study represents a significant step in developing an understanding of the elasticity of the cross-linked polytetrapeptide of elastin.

Fibrous elastin provides the essential elasticity of such tissues as ligaments, lung, skin, and vascular wall. The single soluble precursor protein of fibrous elastin is called tropoelastin[1-3] and has been found to contain repeating sequences—a tetrapeptide (L-Val_1-L-Pro_2-Gly_3-Gly_4), a pentapeptide (L-Val_1-L-Pro_2-Gly_3-L-Val_4-Gly_5), and a hexapeptide (L-Ala_1-L-Pro_2-Gly_3-L-Val_4-Gly_5-L-Val_6).[4-7] Extensive characterizations by physical methods have shown that the monomeric and polymeric forms of these peptides in solution all exhibit a β-turn,[8,9] a ten-membered hydrogen-bonded ring between the C=O of residue-1 and the N–H of residue-4 with Pro_2-Gly_3 at the corners of the β-turn and providing the end peptide moiety with a type II orientation.[10,11] The pentapeptide and hexapeptide repeats can also exhibit a γ-turn, an eleven-membered hydrogen-bonded ring between the Gly_3NH and the Gly_5C=O.[8,9,12,13] Under certain conditions of temperature and solvent, a 14-membered hydrogen bonded ring has also been found to occur.[8,14,15]

Of particular note is that the polytetrapeptide (of interest here) and the polypentapeptide, like tropoelastin and α-elastin[16] (a chemical fragmentation product of fibrous elastin), are each soluble in water in all proportions below 20 °C, but on raising the temperature, they aggregate and, on standing, settling occurs with formation of a dense viscoelastic phase called the coacervate.[9] The process of coacervation is reversible, and the coacervates are about half peptide or protein and half water as is hydrated fibrous elastin. Of interest to the development of an understanding of the mechanism of polypeptide elasticity is that cross-linking, of the polypentapeptide and of the polytetrapeptide of elastin either by chemical means[17] or by γ-irradiation of the coacervates,[18,19] results in elastomeric matrices with striking similarities to fibrous elastin.[20,21] The similarities are with respect to elastic modulus and temperature dependence of elastomeric force.

The studies of conformation and elastic mechanism are well-advanced for the polypentapeptide and the present report of the cyclohexadecapeptide of the polytetrapeptide corresponds to one of the essential steps in the polypentapeptide study. A brief summary of the polypentapeptide studies is given for the purpose of placing the present polytetrapeptide study in perspective.

A key in developing a mechanism for the elasticity of the polypentapeptide (PPP) of elastin was the approach of examining the conformations of cyclic molecules containing from one to six repeating pentamer units and determining which if any of these cyclic structures had a conformation like the linear high polymer. The idea is that a loose helical structure with several repeats per turn could have closely the same set of conformations in one turn as a cyclic molecule or, inversely, that an unstrained cyclic structure containing a substantial number of residues, say ten or more, could be converted to a linear helical conformation of low pitch with only small changes in a few torsion angles.[22] It was found that the cyclopentapeptide and cyclodecapeptide had very different conformations from each other and from the cyclopentadecapeptide but that the cyclopentadecapeptide exhibited a conformation very nearly identical with that of the linear po-

† Current address: Department of Nutrition Sciences, University of Alabama at Birmingham, Birmingham, AL 35294.

(1) Smith, D. W.; Weissman, N.; Carnes, W. H. *Biochem. Biophys. Res. Commun.* **1968**, *31*, 309–315.
(2) Sandberg, L. B.; Weissman, N.; Smith, D. W. *Biochemistry* **1969**, *8*, 2940–2945.
(3) Smith, D. W.; Brown, D. M.; Carnes, W. H. *J. Biol. Chem.* **1972**, *247*, 2427–2432.
(4) Gray, W. R.; Sandberg, L. B.; Foster, J. A. *Nature (London)* **1973**, *246*, 461–466.
(5) Foster, J. A.; Bruenger, E.; Gray, W. R.; Sandberg, L. B. *J. Biol. Chem.* **1973**, *248*, 2876–2879.
(6) Sandberg, L. B.; Gray, W. R.; Foster, J. A.; Torres, A. R.; Alvarez, V. L.; Janaga, J. *Adv. Exp. Med. Biol.* **1977**, *79*, 277–284.
(7) Sandberg, L. B.; Soskel, N. T.; Leslie, J. B. *N. Engl. J. Med.* **1981**, *304*, 566–579.
(8) Urry, D. W.; Long, M. M. *CRC Crit. Rev. Biochem.* **1976**, *4*, 1–45.
(9) Urry, D. W. *Meth. Enzymol.* **1982**, *82*, 673–716.
(10) Venkatachalam, C. M. *Biopolymers* **1968**, *6*, 1425.
(11) Khaled, M. A.; Urry, D. W. *Biochem. Biophys. Res. Commun.* **1976**, *70*, 485–491.
(12) Nemethy, G.; Printz, M. P. *Macromolecules* **1972**, *6*, 755–758.
(13) Khaled, M. A.; Urry, D. W.; Okamoto, K. *Biochem. Biophys. Res. Commun.* **1976**, *72*, 162–169.
(14) Renugopalakrishnan, V.; Khaled, M. A.; Urry, D. W. *J. Chem. Soc., Perkin Trans. 2* **1978**, 111–119.
(15) Khaled, M. A.; Venkatachalam, C. M.; Trapane, T. L.; Sugano, H.; Urry, D. W. *J. Chem. Soc., Perkin II*, **1980**, 1119–1130.
(16) Thomas, J.; Elsden, D. F.; Partridge, S. M. *Nature (London)* **1963**, *200*, 651–652.
(17) Urry, D. W.; Okamoto, K.; Harris, R. D.; Hendrix, C. F. *Biochemistry* **1976**, *15*, 4083–4089.
(18) Urry, D. W.; Harris, R. D.; Long, M. M. *J. Biomed. Mater. Res.* **1982**, *16*, 11–16.
(19) Urry, D. W.; Prasad, K. U. In "Biocompatibility of Natural Tissues and Their Synthetic Analogues"; Williams, D. F., Ed.; CRC Press: Boca Raton, FL, 1985; pp 89–116.
(20) Urry, D. W. *J. Protein Chem.* **1984**, *3*, 403–436.
(21) Urry, D. W.; Venkatachalam, C. M.; Wood, S. A.; Prasad, K. U. In "Structure and Motion: Membranes, Nucleic Acids and Proteins"; Clementi, E., G. Corongiu, G., Sarma, M. H., Sarma, R. H., Eds.; Adenine Press: Guilderland, NY, 1985, pp 185–204.
(22) Urry, D. W. *Proc. Natl. Acad. Sci. U.S.A.* **1972**, *69*, 1610–1614.

0002-7863/85/1507-7139$01.50/0

lypentapeptide, and it did so in different solvents and over the accessible temperature ranges;[23] that is, the cyclopentadecapeptide was found to be the cyclic conformational correlate of the linear PPP. The solution conformation of the cyclopentadecapeptide was developed in detail[24] (in the same manner as reported here for the cyclohexadecapeptide of the repeat tetrapeptide series), and it compared very closely to the independently determined crystal structure of the cyclopentadecapeptide.[25] In the crystal, the three type II Pro-Gly β-turns were found arranged as three feet for the cyclic molecules with one cyclic molecule stacked directly on top of the other; the dominant intermolecular contacts were hydrophobic; the Val_4-Gly_5-Val_1 segment was suspended between β-turns, and the crystal was about one-third water with the water occurring within the stack of cyclic molecules. The cyclic conformation was then computationally converted to the helical linear conformational correlate[26] termed a β-spiral. The β-spiral is so-named because the β-turn is the dominant secondary structural feature and the pentamer conformation recurs as a helical repeat. The β-turns function as spacers between the turns of the helix by means of hydrophobic contacts; there is water within the β-spiral which can exchange with extraspiral water through spaces in the surface of the β-spiral, and connecting the β-turns is a suspended segment, Val_4-Gly_5-Val_1, wherein the peptide moieties have much freedom to rock, i.e., to librate. These librations are viewed as a large source of entropy, and the librations are damped on extension, as would occur on stretching, such that the elastomeric restoring force would be largely entropic.[27] This has been termed a librational entropy mechanism of elasticity.[9,28]

Numerous physical methods have characterized the change in structural state attending formation of the viscoelastic coacervate of the polypentapeptide: (a) temperature dependence of aggregation and associated (light and transmission and scanning electron) microscopic examination of the aggregates demonstrate intermolecular ordering of polypeptide with increasing temperature;[9,27] (b) nuclear magnetic resonance relaxation studies demonstrate an inverse temperature transition;[29] (c) circular dichroism studies show the conversion from a more nearly random state at low temperature to a structure at 40 °C of regularly recurring β-turns;[9,30] (d) dielectric relaxation studies show the development on going from 20 to 40 °C of an intense local Debye-type relaxation at 25 MHz, indicating that each pentamer has developed the same conformation characterized by a common peptide librational mode;[20,31] and (e) thermoelasticity studies on the γ-irradiation cross-linked coacervate state show that the elastomeric force goes from essentially zero at 20 °C, before the transition, to a near maximal value at 40 °C when coacervation is complete.[20,21] Interestingly, the development of the intensity of the 25-MHz dielectric relaxation closely parallels the increase in elastomeric force with temperature[32] as do the temperature dependences of the other physical characterizations which also indicate increase in intra- and intermolecular order with increase in temperature. Accordingly, the data on the polypentapeptide argue that a new mechanism of elasticity is required wherein the relaxed state contains a describable albeit dynamic regularity of structure as opposed to the kinetic theory of rubber elasticity wherein the relaxed state is considered to be totally random.

With respect to the polytetrapeptide of elastin, the present stage is one of describing the solution conformation of a cyclic analogue that is a reasonable cyclic conformational correlate of the linear polytetrapeptide. In the present report are the synthesis and conformational characterization of the cyclohexadecapeptide, *cyclo*-$(VPGG)_4$. The conformational analysis of this cyclic peptide is achieved by combining NMR spectroscopy with theoretical conformational energy calculations. As only ranges of possible values for the torsion angles, ϕ and ψ, are obtained from an analysis of the spin–spin coupling constants, these constraints are utilized in conformational energy calculations to obtain values of ϕ and ψ tortion angles for low-energy conformations that are consistent with the NMR data. The possible cyclic conformations contained the β-turns and become candidates for the development of the β-spiral of the polytetrapeptide which in turn can become a rational basis with which to explore further the mechanism of elasticity of the cross-linked polytetrapeptide.

Materials and Methods

Synthesis. The synthesis of *cyclo*-$(VPGG)_4$ was carried out by the classical solution methods. The monomeric tetrapeptide was synthesized as shown below, the details of which have been reported[33] earlier.

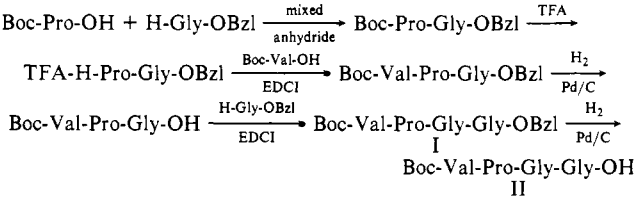

After deblocking I with TFA (trifluoroacetic acid), it was coupled with II using 1-(3-(dimethylamino)propyl)-3-ethylcarbodiimide hydrochloride (EDCI)[34] and 1-hydroxybenzotriazole (HOBt). The octapeptide benzyl ester thus obtained was deblocked and coupled with II to obtain the dodecapeptide benzyl ester which was deblocked and further coupled with II to obtain the protected hexadecapeptide benzyl ester. After hydrogenation, the peptide was converted to *p*-nitrophenyl ester using *p*-nitrophenyl trifluoroacetate.[35] After removing the *tert*-butyloxycarbonyl (Boc) group, cyclization was carried out at a high dilution in pyridine to obtain *cyclo*-$(VPGG)_4$.

All the intermediate peptides were characterized by TLC (thin-layer chromatography), in different solvent systems, ^1H and ^{13}C NMR spectra and elemental analyses. The TLC was performed on silica gel plates supplied by Whatman, Inc., by utilizing the following systems: R_f^1 chloroform/methanol/acetic acid (85:15:3); R_f^2 chloroform/methanol (5.1); R_f^3 *n*-butyl alcohol/acetic acid/water (4:1:1); R_f^4 chloroform/methanol/acetic acid (75:25:3), and R_f^5 *n*-butyl alcohol/acetic acid/water/pyridine (30:6:24:20). Detection of the peptides on TLC plates was with ninhydrin spray and/or chlorine–toluidine reagent. Elemental analyses were carried out by Midwest Microlab Ltd., Indianapolis, IN. Boc-amino acids were purchased from Bachem Inc., Torrence, CA, and EDCI and HOBt were purchased from Aldrich Chemical Co., Milwaukee, WI. The Pro- and Val-amino acids were of the L configuration.

Boc-(Val-Pro-Gly-Gly)$_2$-OBzl (III). To a solution of II (6.2 g, 14.47 mmol) in DMF (35 mL) at ice-cold temperature were added HOBt (2.6 g, 17 mmol) and EDCI (3.26 g, 17 mmol) and stirred for 15 min. To this was added an ice-cold solution of TFA·H-Val-Pro-Gly-Gly-OBzl (obtained by deblocking I with TFA) and triethylamine (Et_3N) (2.37 mL, 17 mmol) in DMF (30 mL). The reaction mixture was stirred at 4 °C overnight and at room temperature for 24 h. After removing DMF, the peptide was taken in $CHCl_3$ and extracted with 20% citric acid, water, saturated $NaHCO_3$ solution, and water and dried over anhydrous $MgSO_4$. The solvent was removed under reduced pressure and the peptide was chromatographed over a silica gel column (4.1 × 52 cm) using 3% methanol in $CHCl_3$ to obtain 8.29 g of the title compound: R_f^1, 0.76, R_f^2, 0.63; R_f^3, 0.75; mp shrinks at 107 °C and melts completely at 124 °C. Anal. Calcd for $C_{40}H_{60}N_8O_{11}$: C, 57.95; H, 7.29; N, 13.51. Found: C, 58.42; H, 7.9; N, 13.13.

Boc-(Val-Pro-Gly-Gly)$_3$-OBzl (IV). After deblocking III, the TFA salt was coupled with II and the dodecapeptide benzyl ester was worked

(23) Urry, D. W.; Trapane, T. L.; Sugano, H.; Prasad, K. U. *J. Am. Chem. Soc.* **1981**, *103*, 2080–2089.
(24) Venkatachalam, C. M.; Khaled, M. A.; Sugano, H.; Urry, D. W. *J. Am. Chem. Soc.* **1981**, *103*, 2372–2379.
(25) Cook, W. J.; Einspahr, H. M.; Trapane, T. L.; Urry, D. W.; Bugg, C. E. *J. Am. Chem. Soc.* **1980**, *102*, 5502–5505.
(26) Venkatachalam, C. M.; Urry, D. W. *Macromolecules* **1981**, *14*, 1225–1229.
(27) Urry, D. W.; Venkatachalam, C. M.; Long, M. M.; Prasad, K. U.; In "Conformation in Biology"; Srinvasan, R., Sarma, R. H., Eds.; Adenine Press: Guilderland, NY, 1982; G. N. Ramachandran Festschrift Volume, pp 11–27.
(28) Urry, D. W. *Ultrastruct. Pathol.* **1983**, *4*, 227–251.
(29) Urry, D. W.; Trapane, T. L.; Iqbal, M.; Venkatachalam, C. M.; Prasad, K. U. *Biochemistry* **1985**, *24*, 5182–5189.
(30) Urry, D. W.; Prasad, K. U.; Trapane, T. L.; Iqbal, M.; Harris, R. D.; Henze, "American Chemical Society Division of Polymeric Materials: Science and Engineering"; Wiley: New York, **1985**; Vol. 53, pp 241–245.
(31) Henze, R.; Urry, D. W. *J. Am. Chem.* **1985**, *107*, 2991–2993.
(32) Urry, D. W.; Henze, Rolf; Harris, R. D.; Prasad, K. U. *Biochem. Biophys. Res. Commun.* **1984**, *125*, 1082–1088.
(33) Urry, D. W.; Ohnishi, T. *Biopolymers* **1974**, *13*, 1223.
(34) Sheehan, J. C.; Preston, J.; Cruickshank, P. A. *J. Am. Chem. Soc.* **1965**, *87*, 2492.
(35) Sakakibara, S.; Inukai, N. *Bull. Chem. Soc. Jpn.* **1964**, *37*, 1231.

up as described for the preparation of III (yield 98%): R_f^1, 0.5; R_f^2, 0.53; R_f^3, 0.64; mp 87–89 °C dec. Anal. Calcd for $C_{54}H_{82}N_{12}O_{15}$: C, 56.92; H, 7.25; N, 14.75. Found: C, 57.10; H, 7.24; N, 14.59.

Boc-(Val-Pro-Gly-Gly)$_4$-OBzl (V). The Boc group was removed from IV and coupled with II to obtain V following the procedure described for III (yield 80%): R_f^1, 0.46; R_f^2, 0.32; R_f^3, 0.53; mp 144 °C (dec). Anal. Calcd for $C_{68}H_{104}N_{16}O_{19}$: C, 56.33; H, 7.23; N, 15.46. Found: C, 55.91; H, 7.3; N, 15.03.

Boc-(Val-Pro-Gly-Gly)$_4$-OH (VI). Compound V (1.5 g, 1.03 mmol) in glacial HOAc (35 mL) was hydrogenated in the presence of 10% Pd/C catalyst at 40 psi. Catalyst was filtered and the solvent removed under reduced pressure. The residue was taken in saturated $NaHCO_3$ solution and extracted with ether. The aqueous solution was cooled and acidified to pH 2 with solid citric acid, and the product was extracted into $CHCl_3$. The $CHCl_3$ extract was washed with saturated NaCl and dried and solvent removed to obtain the title compound (yield 71%): R_f^3, 0.39; R_f^4, 0.08; mp 140 °C dec. Anal. Calcd for $C_{61}H_{98}N_{16}O_{19}$: C, 53.88; H, 7.26; N, 16.48. Found: C, 54.13; H, 7.66; N, 16.04.

Boc-(Val-Pro-Gly-Gly)$_4$-ONP (VII). Compound VI (0.95 g, 0.7 mmol) in pyridine (10 mL) was reacted with *p*-nitrophenyl trifluoroacetate (0.66 g, 2.8 mmol), and the progress of the reaction was monitored by TLC. After the reaction was complete, pyridine was removed and the residue in $CHCl_3$ was extracted with acid and base as described for III. Solvent was removed, and after triturating with petroleum ether, the product was obtained as an amphorous powder (yield 58%): R_f^1, 0.25; R_f^2, 0.23; R_f^3, 0.51; mp 148 °C dec. Anal. Calcd for $C_{67}H_{101}N_{17}O_{21}$: C, 54.34; H, 6.87; N, 16.08. Found: C, 54.08; H, 6.83; N, 16.37. Each of the preceding linear oligomers were examined by proton and carbon-13 nuclear magnetic resonance. By delineation of the end resonances, it was possible to verify that each tetramer addition had indeed occurred and that the product was $n = 4$.

***cyclo*-(Val-Pro-Gly-Gly)$_4$ (VIII).** Compound VII was treated with TFA for 30 min, and the residue after removing TFA was triturated with ether, filtered, washed with ether, and dried. The TFA salt (0.5 g, 0.33 mmol) was taken in DMF (40 mL) and glacial acetic acid (2 mL) and added to pyridine (1.6 L) at 85–90 °C over a period of 6–8 h and stirred overnight. After removing the solvent, the residue in a mixture of methanol and water (1:1) was passed through a column of mixed-bed resin, eluting with the same solvent system. After removing the solvent, the peptide was chromatographed on an LH-20 column using methanol for elution. All the fractions showing a single spot were combined, concentrated, and lyophilized from water to give 376 mg of *cyclo*-(VPGG)$_4$ (yield 90.6%): R_f^3, 0.41; R_f^4, 0.58; R_f^5, 0.64. Anal. Calcd for $C_{56}H_{88}N_{16}O_{16}$: C, 54.17; H, 7.14; N, 18.05. Found: C, 54.17; H, 7.30; N, 17.60. The molecular weight of the cyclohexadecapeptide calculates to be 1240 daltons. Since the cyclization the only significant possibilities are $n = 4$ and 8, vapor-pressure osmometry (Corona Wescan, Model 232A) was carried out in methanol (1.2 mg/mL) at 30 °C and the experimental estimate of molecular weight was 1350. This demonstrates that the desired cyclohexadecapeptide was obtained at greater than a mole fraction of 0.9.

NMR Measurements. A 10 mM solution of *cyclo*-(VPGG)$_4$ was made in both the CD_3OD and CD_3OH solvents for ^1H NMR measurements while a 30 mM solution was made in CD_3OD and Me_2-SO-d_6 solvents for ^{13}C NMR measurements. Deuterated methanol, CD_3OD, was purchased from Thompson Packard, Inc., while CD_3OH and Me_2-SO-d_6 were purchased from Merck, Sharp & Dohme of Canada.

All the ^1H NMR spectra were obtained on a Varian HR-220 spectrometer. Proton decoupling was done by the field-sweep method using a sideband generated by a Hewlett-Packard Model 5103-A frequency synthesizer. In order to facilitate the ABX spin analysis of the glycyl methylene protons, simulated spectra were obtained with the SS-100 computer system by using a Varian Data Machine spin simulation program.

^{13}C NMR experiments were performed on a JEOL FX-100 spectrometer equipped with a multinuclear probe operating at 25.0 MHz. A 10-μs pulse width was used for a 45° magnetization vector with a 2.5-s repetition time. Multiple selective irradiations were accomplished by using a multiirradiation accessory, JEOL Model 1-MI. In all the selective decoupling experiments, the amplitude of the irradiating field, $\gamma_{1H}H_{irr}/2\pi$ was about 10 Hz. T_1 values for the ^{13}C nuclei were measured by using the inversion–recovery method (180–τ–90 pulse sequence). Four to five data points were used to calculate each T_1 value by the least-squares method.

Conformational Energy Calculations. As discussed later, the NMR data show that within the time scale of observation, *cyclo*-(VPGG)$_4$ exhibits 4-fold symmetry with no significant amount of cis Val-Pro bond observed. This greatly simplifies the conformational analysis. While this symmetry element markedly reduces the number of degrees of freedom of the molecule to that of the tetramer repeat unit, VPGG, a further reduction by 2 of the total number of independent torsion angles occurs due to the conditions of the cyclization with the 4-fold symmetry.[36]

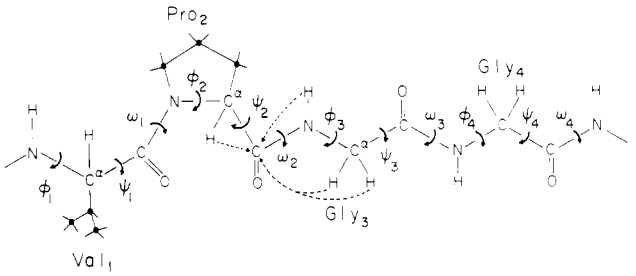

Figure 1. Schematic drawing of the tetramer sequence of elastin defining all torsion angles ϕ_i, ψ_i, and ω_i. Dashed arrows show representative carbon···proton interactions relevant to NMR analyses presented here.

Figure 1 shows a schematic drawing of the tetramer unit, VPGG, where the skeletal backbone torsion angles ϕ_i, ψ_i, and ω_i have been marked.[37,38] When the standard bond lengths and bond angles[39] and planar *trans*-peptide units with all $\omega_i = 180°$ are used, the backbone conformation of the repeat unit, VPGG, is defined by specifying the values of the four pairs of ϕ_i and ψ_i, a total of eight variables. As shown by Go and Scheraga,[36] two torsion angles have to be adjusted to ensure exact cyclization with the 4-fold symmetry. Adjusting ϕ and ψ at Gly$_4$ to meet the conditions of cyclization, only six independent torsion angles are required to explore the conformational space of the molecule. Further, the proline ring closure restricts the value of ϕ_2 to be about −60° and the interaction between Val$_1$ and Pro$_2$ side chains somewhat limits the range of variability of ψ_i. Also, as discussed later, NMR analysis provides ranges of torsion angles (see Figure 6 below). The six independent torsion angles ϕ_1, ψ_1, ϕ_2, ψ_2, ϕ_3, and ψ_3 are varied within the acceptable ranges obtained from NMR, and for each set of these angles, the cyclization conditions[36] are solved to obtain the corresponding values of ϕ_4 and ψ_4, leading to exact cyclization. The valyl side chain is initially fixed at the ideal "trans" conformation with $\chi(H^\alpha–C^\alpha–C^\beta–H^\beta) = 180°$,[37] and the proline ring is then fixed in the "down" γ-puckered ring structure.[39] The total conformational energy of the cyclic peptide is calculated for each cyclic conformation so obtained, using the potential functions of Scheraga and co-workers.[39,40] This results in a set of low-energy conformations which are then refined by complete energy minimization by using Fletcher's algorithm[41] with respect to the six independent torsion angles, with ϕ_4 and ψ_4 being adjusted within the algorithm to preserve cyclization during minimization. During the later stages of the minimization iterations, the valyl side chain torsion angle χ_1^1 was allowed to depart from its ideal value, corresponding to the perfectly staggered conformation about the $C^\alpha–C^\beta$ bond. Since the valyl side chain plays an important role in the conformational stability of this repeat peptide, calculations are repeated by using the two gauche conformations of the valyl side chains. The results are expected to delineate the role of the valyl side chain in this molecule.

Results

NMR Spectral Studies. The ^1H NMR resonances of the three amino acid residues, namely valine, proline, and glycine, can easily be recognized from their splitting patterns which are presented in Figure 2. For example, both valine and proline appear as pseudotriplets in Figure 2A. On prior exchanging of the peptide N*H* proton, Figure 2B shows the valine α-C*H* proton as a doublet. However, assignment of the two glycine residues, Gly$_3$ and Gly$_4$, cannot be made unambiguously in this way.

This laboratory has demonstrated the combined use of ^1H and ^{13}C spectra, each observed during the selective decoupling of ^1H resonances, which allows simultaneous assignment of both the ^1H and ^{13}C resonances of peptides.[42,43] The basic principle of this technique is to selectively irradiate the α-H$_i$ and NH$_{i+1}$ protons,

(36) Go, N.; Scheraga, H. A. *Macromolecules* **1973**, *6*, 273.
(37) IUPAC-IUB Recommendations *J. Mol. Biol.* **1970**, *52*, 1.
(38) Ramachandran, G. N.; Sasisekharan, V. *Adv. Protein Chem.* **1968**, *23*, 283.
(39) Momany, F. A.; Carruthers, L. M.; McGuire, R. F.; Scheraga, H. A. *J. Phys. Chem.* **1974**, *78*, 1595.
(40) Momany, F. A.; McGuire, R. F.; Burgess, A. W.; Scheraga, H. A. *J. Phys. Chem.* **1975**, *79*, 2361.
(41) Fletcher, R. Report R7125, AERE, Harwell.
(42) Khaled, M. A.; Urry, D. W. *J. Chem. Soc., Chem. Commun.* **1981**, 230.
(43) Khaled, M. A.; Harris, R. D.; Prasad, K. U.; Urry, D. W. *J. Magn. Reson.* **1981**, *44*, 255.

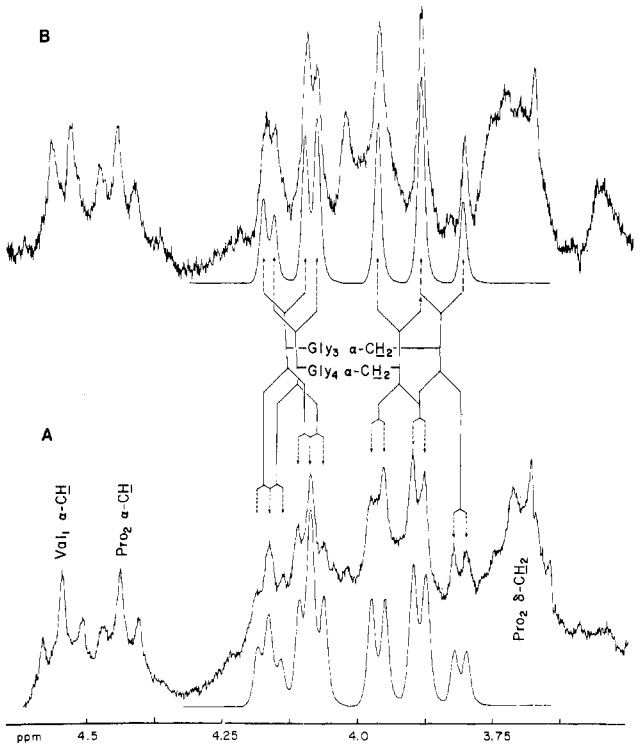

Figure 2. ^{1}H NMR spectra (220 MHz) (α-proton region only) of *cyclo*-(VPGG)$_4$ (A) in CD_3OH and (B) in CD_3OD.

across a peptide bond, which are ^2J-coupled to the C_i=O carbon. This is shown by arrows in Figure 1. These two protons also provide almost all of the nuclear Overhauser enhancement (NOE) for the C_i=O carbon. Once two such protons are located and one of the residues is identified, either from its side chain pattern or by perturbing the end groups in the case of a linear peptide, the rest of the residues in the molecule can be assigned by stepwise irradiation of the ^{1}H resonances.

Inspection of the repeat sequence in Figure 1 indicates that the Gly$_3$N*H* proton is ^2J-coupled to the Pro$_2$C=O carbon. Selective irradiation of the lowest field Gly N*H* proton at 8.55 ppm sharpens the lowest field C=O carbon resonance at 173.03 ppm as shown in Figure 3D (compare Figure 3C and D). Simultaneous irradiation of the same Gly N*H* proton and also of the Pro$_2$ α-C*H* proton at 4.43 ppm further reduces the line width of the same carbonyl carbon at 173.03 ppm (see Figure 3E). Note that the Val$_1$ C=O carbon at 171.19 ppm appears very sharp since it is devoid of the ^2J coupling with an N*H* proton because proline, an N-substituted amino acid, is the subsequent residue. This is consistent with the previous findings[14] in *cyclo*-(VPGVG)$_2$. Since the C=O carbon signal at 173.03 ppm is ^2J-coupled to Pro$_2$$\alpha$-C*H*, it is, therefore, assigned to the Pro$_2$ C=O carbon. However, the line width of the Pro$_2$ C=O carbon is not as narrow as one would expect (compare Figure 3B and E). This could be due to the ^3J coupling to the Gly$_3$CH_2 protons.

The above-mentioned difficulty can be eliminated by measuring the selective ^{13}C–^{1}H NOE as indicated earlier.[44] Figure 3F shows the C=O carbon resonances obtained by broad-band decoupling of all the proton resonances but without NOE (no NOE gated decoupling). Figure 3G is the result of the same experiment but with the selective saturation of the lowest field Gly$_3$ N*H* proton at 8.55 ppm. The difference spectrum, depicted in Figure 3H, exhibits only the Pro$_2$ C=O carbon resonance at 173.03 ppm. Selective heteronuclear NOE, therefore, seems to be a convenient method for the ^{1}H and ^{13}C signal assignments. Since the Gly N*H* proton signal at 8.55 ppm is, thus, assigned to the Gly$_3$ residue, the other Gly N*H* proton at 8.21 ppm, by elimination, is, therefore, assigned to the Gly$_4$ residue. Selective irradiation of this Gly$_4$ N*H* proton delineated the Gly$_3$ C=O carbon at 170.12 ppm from the Gly$_4$ C=O carbon resonance at 169.49 ppm since the Gly$_4$ N*H* proton is ^2J-coupled to the Gly$_3$ C=O carbon (see Figure 1). Having made all the assignments, the ^{1}H NMR parameters so obtained are listed in Table I and ^{13}C NMR parameters in Tables II and III.

Table I. ^{1}H NMR Parameters of *cyclo*-(VPGG)$_4$ in Methanol

parameters	residues			
	L-Val$_1$	L-Pro$_2$	Gly$_3$[a]	Gly$_4$[a]
Chemical Shifts (δ), ppm (±0.01)				
N*H*	7.98		8.55	8.21
C$^\alpha$*H*	4.55	4.43	3.89, 4.14	3.93, 4.12
C$^\beta$*H*	*b*	*b*		
C$^\gamma$*H*	1.0, 1.04	*b*		
C$^\delta$*H*		3.69		
Coupling Constants (J), Hz (±0.25)				
$^3J_{NH-C^\alpha H}$	8.0		5.0, 6.0	5.0, 5.0
$^3J_{C^\alpha H-C^\beta H}$	7.5	7.0		
$^3J_{C^\beta H-C^\gamma H}$	6.5	*c*		
$^2J_{HH}$			−17.0	−17.5
Temperature Coefficient, ($\Delta\delta/\Delta T$), ppm/°C × 10^{-3}				
peptide N*H*	−6.26		−6.11	−3.13

[a] Values for the two glycine residues were obtained by ABX spin simulation. [b] Overlapped between 1.82 and 2.27 ppm. [c] Not analyzed.

The first step in the structural evaluation of a peptide is to find out if there is any hydrogen bond formed within the molecule. Generally, two ^{1}H NMR methods are used to detect H-bonded (solvent-shielded) peptide N*H* protons. These are the temperature dependence of the peptide N*H* protons and the solvent dependence (from basic to protic solvents) of the chemical shifts of the peptide N*H* protons.[45,46] The peptide N*H* proton chemical shift variation, $\Delta\delta$, is monitored as a function of temperature. The numerical values of temperature coefficient ($\Delta\delta/\Delta T$) obtained in MeOH are included in Table I, and the graphical representations are given in Figure 4. The peptide N*H* proton solvent shift ($\Delta\delta/\Delta S$) from the weakly basic solvent, Me_2SO-d_6, to the protic solvent, trifluoroethanol (TFE), was followed. In order to relate the structural behavior in MeOH, a similar solvent titration from MeOH to TFE was also followed. These are presented in Figure 5.

^{13}C NMR has also been utilized to delineate the intramolecularly H-bonded peptide C=O groups.[8] The chemical shifts of an exposed C=O carbon vary markedly on going from a basic solvent, e.g., Me_2SO-d_6 to a protic solvent, e.g., water. Solvent titrations of the carbonyl carbon resonances of *cyclo*-(VPGG)$_4$ were, therefore, performed, and the results are summarized in Table II. The solvent shifts are listed both as the change in chemical shift with change of solvent ($\Delta\delta/\Delta S_{ij}$) and as the change in chemical shift ($\Delta\delta_{m1}$) calculated with respect to the carbonyl carbon resonance which showed the lowest downfield shift. Table II also contains the similar ^{13}C NMR parameters for the linear polytetrapeptide, (VPGG)$_n$, for the purpose of comparing the spectral behavior between the cyclic and the linear (VPGG) fragments.

It can be noticed in Figure 2 that the Gly$_3$ CH_2 protons are more nonequivalent than the Gly$_4$ CH_2 protons. This may be due to the increased flexibility at the Gly$_4$ position. Spin–lattice relaxation time (T_1) studies were carried out to access such flexibility in *cyclo*-(VPGG)$_4$. T_1 values obtained in CD_3OD are given in Table III.

Conformational Energy Calculations. When the six independent torsion angles are varied within the acceptable ranges obtained from NMR (Figure 6), successful cyclization resulted in several hundreds of sets of angles. About 2000 cyclic structures were obtained. Energy calculations with a trans valyl side chain gave several low-energy conformations. Most of the resulting torsion

(44) Khaled, M. A.; Watkins, C. L. *J. Am. Chem. Soc.* **1983**, *105*, 3363.

(45) Kopple, K. D.; Ohnishi, M.; Go, A. *J. Am. Chem. Soc.* **1969**, *91*, 4264.

(46) Ohnishi, M.; Urry, D. W. *Biochem. Biophys. Res. Commun.* **1969**, *36*, 194.

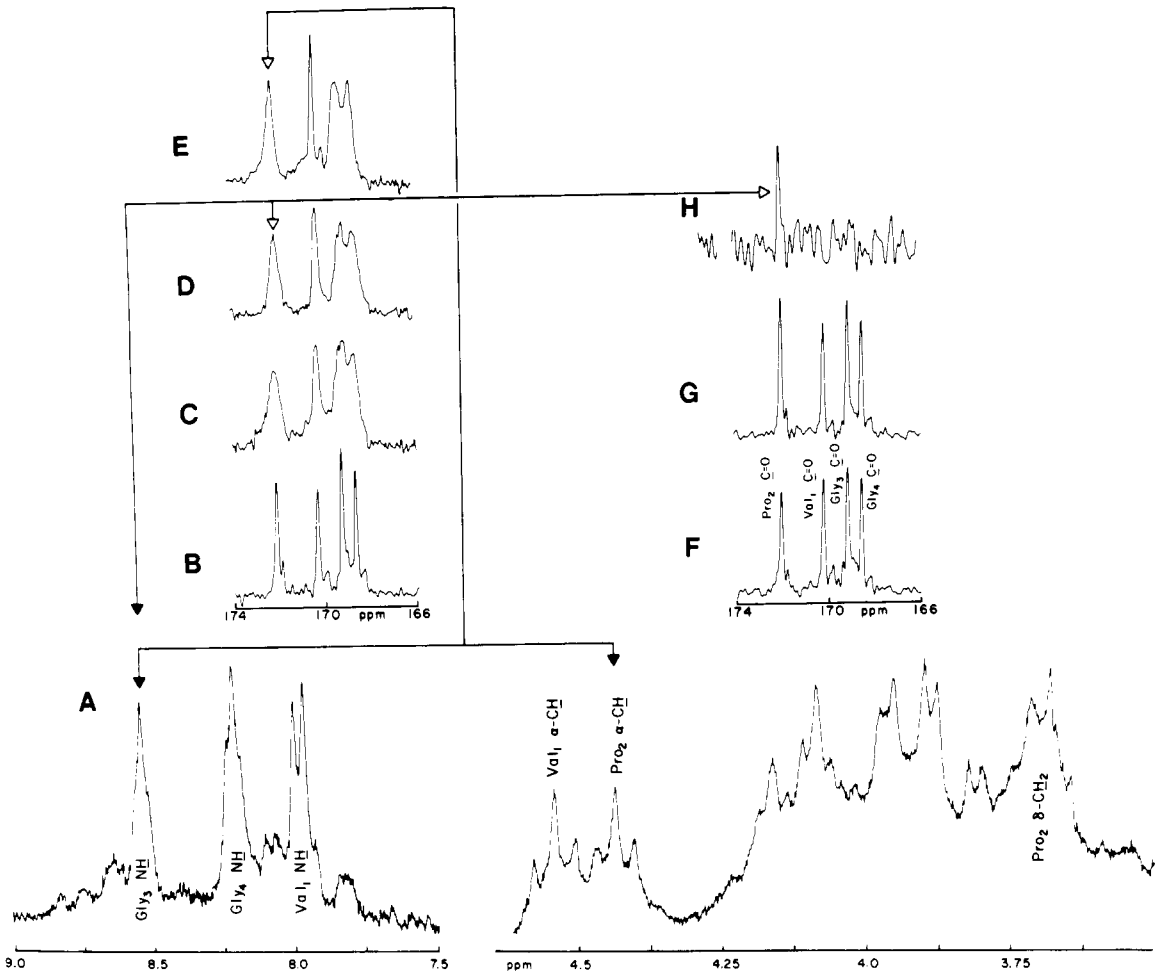

Figure 3. Selective irradiation experiment: (A) 220-MHz ^1H spectrum of *cyclo*-(VPGG)$_4$ in CH_3OH (α- and N*H* proton regions only); (B–H) 25-MHz ^{13}C NMR of *C*=O carbons of *cyclo*-(VPGG) in CD_3OH. (B) broad-band ^1H irradiation with NOE, (C) ^1H undecoupled, (D) Gly_3 N*H* proton selectively irradiated, (E) both Gly_3 N*H* and Pro_2 C$^\alpha$*H* protons selectively decoupled, (F) broad band proton decoupled *without NOE*, (G) same as F *with NOE*, and (H) difference spectrum obtained by subtracting F from G. Note that the irradiated resonances are indicated by the filled triangles (▲), while the observed signals are indicated by the open triangles (△).

Table II. Solvent Shifts ($\Delta\delta/\Delta S$)[a] of the Carbonyl Carbon Resonances

	cyclo-(VPGG)$_4$				H-(VPGG)$_n$-Val-OMe			
residue	Me_2SO-d_6	D_2O	$\Delta\delta/\Delta S$	$\Delta\delta_{m1}$[b]	Me_2SO-d_6	D_2O	$\Delta\delta/\Delta S$	$\Delta\delta_{m1}$[b]
Val_1C=O	171.18	172.84	1.66	0	171.04	172.84	1.80	0
Pro_2C=O	173.03	174.60	2.57	0.91	172.99	175.56	2.57	0.77
Gly_3C=O	170.12	172.84	2.72	1.06	170.02	172.69	2.67	0.87
Gly_4C=O	169.49	171.72	2.23	0.57	169.44	171.67	2.23	0.43

[a] Solvent shift ($\Delta\delta/\Delta S$) from Me_2SO to D_2O, expressed in ppm. [b] $\Delta\delta_{m1} = (\Delta\delta/\Delta S_{ij})_m - (\Delta\delta/\Delta S_{ij})_1$ where *m* stands for the *m*th residue and 1 for residue 1; i.e., the residue 1 carbonyl carbon resonance is used as an internal reference since it exhibited the least solvent dependence.

Table III. ^{13}C NMR Parameters of *cyclo*-(VPGG)$_4$ in Methanol

residue	C atoms	chem shifts, ppm	spin–lattice relaxation time (T_1), s
Val_1	C^α	62.27	0.174
	C^β	31.79	0.207
	C^γ	19.66, 18.78	1.288, 1.814
	C=O	172.50	2.589
Pro_2	C^α	58.05	0.161
	C^β	30.34	0.267
	C^γ	26.31	0.399
	C^δ	*a*	*a*
	C=O	174.93	2.603
Gly_3	C^α	43.29	0.190
	C=O	172.11	2.305
Gly_4	C^α	43.78	0.208
	C=O	171.38	2.179

[a] Overlapped with the solvent peaks.

angles are found to be generally within or near the acceptable ranges. The values of ϕ and ψ at Gly_4 were found to show considerable variation among the low-energy structures. The lowest energy structure exhibits a trans valyl side chain. Higher conformational energies are obtained if the valine side chain is fixed in the gauche conformations. The torsion angles of six low-energy structures are listed in Table IV, and Figure 7 depicts their stereoviews.

Discussion

The appearance of a single NMR resonance for a particular nucleus or group of equivalent nuclei would be indicative either of a single, well-defined conformation of the molecule or of a set of rapidly interconverting structures. It can be noticed in Figure 3, particularly in the N*H* proton and the C=O carbon regions, that there are additional detectable weak signals. These additional signals could be due to either a cis–trans isomerism at the Val_1-Pro_2 peptide bond, as was observed in *cyclo*-(VPG)$_2$,[47] or due to a conformation which does not maintain a 4-fold symmetry for

(47) Khaled, M. A.; Renugopalakrishnan, V.; Sugano, H.; Rapaka, R. S.; Urry, D. W. *J. Phys. Chem.* **1978**, *82*, 2743.

Table IV. Torsion Angles of the Low Structures of *cyclo*-(VPGG)$_4$

	Val_1		Pro_2		Gly_3		Gly_4		
struct	ϕ	ψ	ϕ	ψ	ϕ	ψ	ϕ	ψ	E, kcal/mol
A	−86	122	−60	140	138	−38	55	87	21.6
B	−90	120	−60	122	121	35	−87	180	22.7
C	−87	126	−60	125	142	−36	63	111	23.8
D	−114	88	−60	155	99	37	−110	−132	23.9
E	−150	121	−60	138	101	−39	81	−177	27.2
F	−60	150	−60	160	138	−37	−68	120	28.3

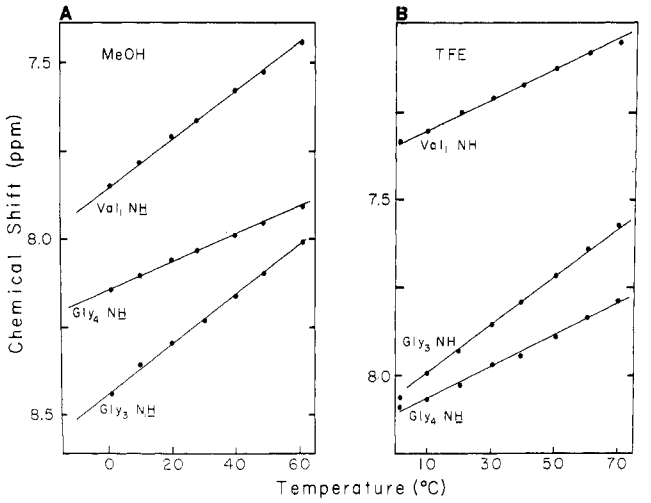

Figure 4. Temperature dependence of peptide N*H* protons of *cyclo*-(VPGG)$_4$: (A) in CD_3OH and (B) in TFE.

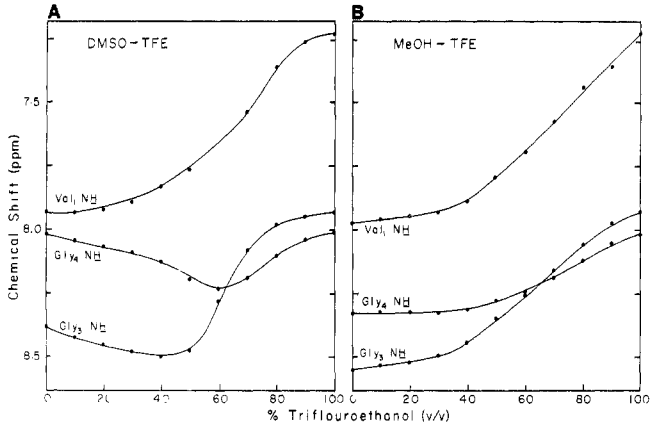

Figure 5. Solvent shifts of peptide N*H* protons of *cyclo*-(VPGG)$_4$: (A) from Me_2SO-d_4 to TFE and (B) from CD_3OH to TFE.

cyclo-(VPGG)$_4$ in solution. We are, however, concerned with the major form of the molecule giving the most intense signals (see Figure 2) which indicate that this form of the molecule retains the 4-fold symmetry in solution within the 220-MHz NMR time scale.

When a peptide N*H* proton is involved in an energetically most favorable interaction with the C=O oxygen and/or in a close contact with any other atoms within the molecule, it shows low-temperature dependence of its chemical shift. From the temperature studies of the peptide N*H* proton chemical shifts of *cyclo*-(VPGG)$_4$ in MeOH and TFE, as shown in Figure 4, it appears that the Gly_4N*H* is least shifted. The temperature coefficients ($\Delta S/\Delta T$), tabulated in Table I, also show that the Gly_4 N*H* proton gives a $\Delta\delta/\Delta T$ of -3.13×10^{-3} ppm/°C, while the Val_1 N*H* and Gly_3 N*H* protons give values of −6.26 and 6.11 $\times 10^{-3}$ ppm/°C, respectively. This indicates that the Gly_4NH group is well-shielded while Val_1 and Gly_4 N*H* groups are highly exposed.[8]

It can be seen in Figure 5 that both Val_1 and Gly_3 N*H* protons show upfield shifts, whereas the Gly_4 N*H* proton does not show

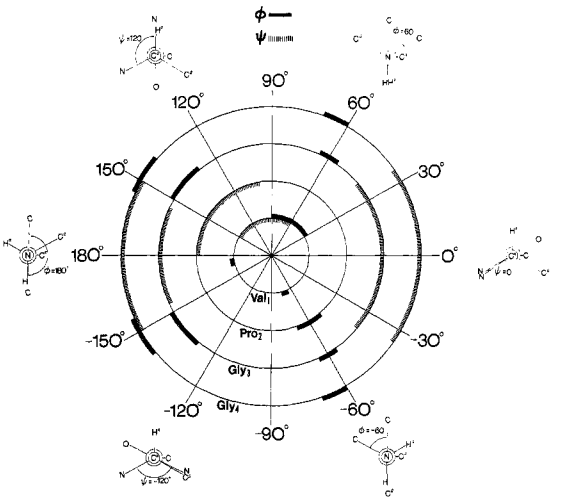

Figure 6. Possible ranges of the backbone torsion angles consistent with the observed NMR coupling constants depicted here by using a polar representation for the torsion angles. The solid regions refer to the torsion angles ϕ and the hatched regions to the angles ψ. Newman projections for typical angular values are also shown to facilitate the examination of these ranges and to make apparent the convention used.

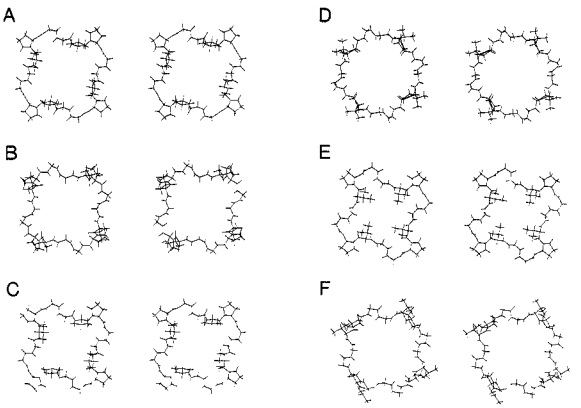

Figure 7. Stereoplots of the low-energy structures obtained from conformational energy calculations. The torsion angles and energies of these structures are given in Table IV.

any appreciable chemical shift change on going from Me_2SO-d_6 to TFE (Figure 5A) and from MeOH to TFE (Figure 5B). In the Gramicidin S model system, the exposed N*H* proton gave an upfield shift of about 1 ppm by the variation of solvents.[48] On the basis of this criterion, the Val_1 and Gly_3 NH groups are, therefore, solvent-exposed, while the Gly_4 N*H* is solvent-shielded.

Comparison of the shielding of the peptide NH group with that of the peptide C=O group provides information on the H-bond pair, i.e., the NH···O=C pairing. In the ^{13}C NMR experiments, the solvent shifts of peptide *C*=O carbons obtained in the Me_2SO/water solvent are listed in Table II. It can be seen that the Val_1 C=O carbon is least-shifted, 1.66 ppm, compared to all other peptide *C*=O carbons. This means that the Val_1 C=O is most involved in intramolecularly H-bonding interaction. In-

(48) Pitner, T. P.; Urry, D. W. *J. Am. Chem. Soc.* **1972**, *94*, 1399.

terestingly, the $\Delta\delta/\Delta S$ values of peptide C=O carbons in *cyclo*-$(VPGG)_4$ are very similar, within the experimental error, to those of linear polytetrapeptide $(VPGG)_n$ (see Table II). As mentioned earlier, the linear VPGG molecule gave rise to a 10-membered H bond, β-turn (type II), between the Val_1 C=O and the Gly_4 NH groups. It is also apparent here in *cyclo*-$(VPGG)_4$ that the same β-turn, with Pro_2-Gly_3 forming the end peptide moiety, is the main conformational feature. Further conformation of this is that the cyclohexadecapeptide and the linear polytetrapeptide exhibit similar β-turn CD patterns.[49]

The conformational torsion angle, ϕ, can be estimated from the observed $^3J_{NH\text{-}C^\alpha H}$ coupling constants.[50] Each $^3J_{NH\text{-}C^\alpha H}$ value can give four possible ranges of the ϕ torsion angles. The ranges of the ϕ torsion angles for Val_1, Gly_3, and Gly_4, obtained from their $^3J_{NH\text{-}C^\alpha H}$ coupling values (see Table I), are presented in Figure 6. The ranges of the torsion angles, ψ, can be obtained from the observed $^2J_{(HH)}$ coupling for the two glycine residues only.[51] They are also shown in Figure 6. Measurement of NOE between the $C^\alpha H_i$ and the NH_{i+1} protons across a peptide can also provide information on the torsion angle, ψ, for residue i.[11,52] For example, the observed NOE between the Pro_2 $C^\alpha H$ and the Gly_3 NH protons could provide the value for ψ_2 of Pro_2. Unfortunately, such experiments could not be performed at 100 MHz because the intense solvent CD_3OH proton signals mask the α-^{1}H region.

For a cyclic molecule of this size with only one hydrogen bond per repeat unit, conformational flexibility is expected. This is evident from examination of wire models and from the conformational energy calculations. This molecular flexibility is also apparent from the T_1 values of all the α-C atoms. An identical T_1 value for all the α-carbons is expected to be seen for a rigid molecule which rotates isotropically in solution.[53] The T_1 values for *cyclo*-$(VPGG)_4$ (see Table III) show that the Val_1 α-C carbon has a higher T_1 (0.174 s) than the Pro_2 α-C (T_1 = 0.161 s), and similarly the Gly_4 α-C carbon T_1 (0.208 s) is higher than that of the Gly_3 α-C carbon (0.190 s). It is appreciated that glycine with two α-protons usually gives higher T_1 values, but it appears that Gly_4 is more flexible than Gly_3. This is also consistent with the observed smaller nonequivalency of its methylene (CH_2) protons (see Figure 2). The $^3J_{NH\text{-}C^\alpha H}$ coupling value of 8.0 Hz for the Val_1 residue also allows for some rotation at the N-C^α bond of this residue which is consistent with its higher T_1 value compared to T_1 of Pro_2 α-C carbon (see Table III). A reasonable explanation of these observations is that *cyclo*-$(VPGG)_4$ contains the β-turn (type II) placing the Pro_2-Gly_3 fragment within the turn and thus rendering these two residues more rigid. On the other hand, the Val_1 and Gly_4 residues are much more flexible, giving rise to appreciable librational freedom for the Gly_4-Val_1 peptide unit.

The flexibility of this molecule is also demonstrated by the existence of several minimum energy structures that are found from the conformational energy calculations. Many of these low-energy structures are similar to each other, and hence it suffices to show a handful of representative structures. These are given in Figure 7. Comparison of the torsion angles of these structures with the NMR-derived ranges in Figure 6 shows satisfactory agreement in general. Some discrepancies may be seen particularly in the values of ϕ_4, ψ_4, and ϕ_1. The absence of an exact agreement between the torsion angles of the low-energy structures with *all* the NMR ranges suggests that conformational averaging is occurring in this molecule.

The structural analysis is, therefore, that the cyclohexadecapeptide contains four repeating β-turns and that the chain segments connecting the β-turns are highly flexible. The result for this cyclic conformational correlate of the polytetrapeptide is quite analogous to that of the cyclopentadecapeptide[24] which is the cyclic conformational correlate of the polypentapeptide[23] and which is the basis for the development of the dynamic β-spiral of the polypentapeptide.[26] Several polypentapeptide β-spirals are considered to supercoil to form the 5.5-nm twisted filaments observed in the transmission electron microscope.[27] The heat-elicited aggregation of the polytetrapeptide results in the observation (in the transmission electron microscope of negatively stained aggregates) of twisted filaments with a width of about 5 nm.[54] The twisted filaments are taken as the fundamental structural unit within the viscoelastic coacervate of the polytetrapeptide, and it is γ-irradiation cross-linking of the polytetrapeptide coacervate that results in the formation of an elastomeric matrix.[18] As a β-spiral structure forms on raising the temperature in water,[54] one looks to intramolecular hydrophobic association, optimized as interturn hydrophobic interactions, to be the structural force leading to β-spiral formation. Also, as the temperature required for coacervation decreases with increasing polytetrapeptide concentration, hydrophobic intermolecular interactions are the dominant process in the formation of the twisted filaments from association of β-spirals. These intramolecular and intermolecular hydrophobic interactions become the guiding principles for utilizing the conformations in Figure 7 to develop the β-spiral of the polytetrapeptide and to develop the twisted filaments.

With respect to the mechanism of elasticity, the flexible chain segment connecting the β-turns and involving the sequence of torsion angles—ϕ_4, ψ_4, ϕ_1—becomes the focal point for the source of librational entropy for the polytetrapeptide β-spiral. The flexibility and librational entropies, in analogy to the β-spiral of the polypentapeptide,[27,28] are expected to decrease on extension of the polytetrapeptide β-spiral. Entropy is then expected to provide a significant component of the elastomeric force of the cross-linked polytetrapeptide.

Acknowledgment. This work was supported in part by the National Institutes of Health, Grant HL-29578.

Registry No. I, 79252-56-5; II, 53488-00-9; III, 98509-19-4; IV, 98509-20-7; V, 98509-21-8; VI, 53488-05-4; VII, 98509-22-9; VIII, 53533-24-7; H-Val-Pro-Gly-Gly-OBzl·TFA, 98509-24-1; H-(Val-Pro-Gly-Gly)$_2$-OBzl·TFA, 98509-26-3; H-(Val-Pro-Gly-Gly)$_4$-ONP·TFA, 98509-28-5.

(49) Urry, D. W.; Long, M. M.; Ohnishi, T.; Jacobs, M. *Biochem. Biophys. Res. Commun.* **1974**, *61*, 1427–1433.
(50) Bystrov, V. F.; Portnova, S. L.; Tsetlin, V. I.; Ivanov, V. T.; Ovchinnikov, Yu A. *Tetrahedron* **1969**, *25*, 439.
(51) Barfield, M.; Hruby, V. J.; Meraldi, J. P. *J. Am. Chem. Soc.* **1976**, *98*, 1308.
(52) Roques, B. P.; Rao, R.; Marion, D. *Biochimie* **1980**, *62*, 753.
(53) Allerhand, A.; Komoroski, R. A. *J. Am. Chem. Soc.* **1973**, *95*, 8228.
(54) Long, M. M.; Rapaka, R. S.; Volpin, D.; Pasquali-Ronchetti, I.; Urry, D. W. *Arch. Biochem. Biophys.* **1980**, *201*, 445–452.